ACS Macro Letters

Letter

pubs.acs.org/macroletters

Decoupling Bulk Thermodynamics and Wetting Characteristics of Block Copolymer Thin Films

Sangwon Kim,[†] Paul F. Nealey,[‡] and Frank S. Bates*[,†]

[†]Department of Chemical Engineering and Materials Science, University of Minnesota, Minneapolis, Minnesota 55455, United States

[‡]Department of Chemical and Biological Engineering, University of Wisconsin, Madison, Wisconsin 53706, United States

Supporting Information

ABSTRACT: The consequences on certain physical properties of controlled levels of epoxidation of the poly(isoprene) blocks in poly(styrene-*b*-isoprene) (PS-PI) diblock copolymers and poly(isoprene) (hPI) homopolymers have been studied, where the products after epoxidation are denoted PS-PIxn and hPIxn, respectively. The effective interaction parameters χ_{eff} between the PS and the PIxn blocks were estimated by applying mean-field theory to the lamellar periodicities identified by small-angle X-ray scattering and to the order-to-disorder transition temperatures determined by dynamic mechanical spectroscopy. These results were fit to a binary segment−segment interaction parameter model indicating a nonlinear change in χ_{eff} with percent epoxidation. In contrast, contact angle measurement on hPIxn and lamellar orientations of thin-film PS-PIxn suggest that the surface energy of PIxn increases linearly with epoxidation. This decoupling of bulk and thin-film thermodynamic behaviors is attributed to the different roles that a random copolymer architecture plays in establishing three-dimensional order versus wetting at a two-dimensional surface.

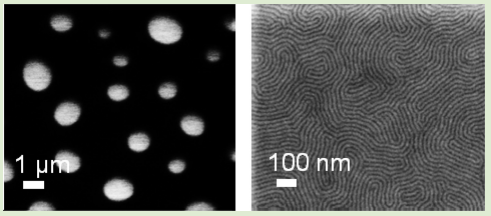

Random copolymer molecular architectures offer versatile strategies for continuously tuning a host of physical properties, either through copolymerization or chemical modification, often with significant commercial implications.[1,2] Block copolymers form myriad morphologies depending on the volume fraction of the constituent blocks, the associated interaction parameters, the overall degree of polymerization, and the molecular architecture.[3] Selective modification of polydiene blocks by fluorination,[4,5] hydrogenation,[6] epoxidation,[7] and liquid crystal attachment[8] have demonstrated that block copolymer phase behavior can be "tuned" by chemical modification. Partial epoxidation of poly(styrene-*b*-isoprene) (PS-PI) dibock copolymers represents a particularly powerful[7,9,10] approach, with distinctly different consequences on bulk and thin film morphologies as demonstrated in this letter.

Poly(styrene) (hPS, M_n = 21.6 kg/mol) and poly(isoprene) (hPI, M_n = 20.1 kg/mol) homopolymers and a symmetric poly(styrene-*b*-isoprene) (PS-PI) diblock copolymer (M_n = 22.8 kg/mol, M_w/M_n = 1.05) were synthesized using anionic polymerization.[4] Specified degrees of partial epoxidation (xn) were attained by reaction with dimethyl dioxirane[11] (without using a phase transfer catalyst), and the products are denoted hPIxn and PS-PIxn (Figure 1). We assume that the epoxidation reaction occurs at random positions along the polymer chains.[12,13]

Small-angle X-ray scattering (SAXS) was employed at room temperature to determine the bulk morphology and domain dimensions for PS-PIxn (Figure 2). Diffraction peaks occur at integer multiples of the principle wavevector $\mathbf{q}_1$ for all specimens, except for PS-PI14 and PS-PI41, indicative of lamellar morphologies as anticipated based on the symmetric

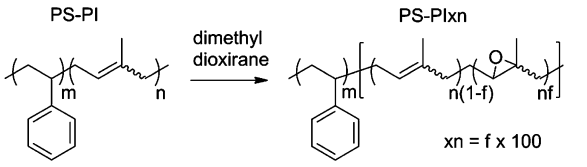

Figure 1. Epoxidation of PS-PI diblock copolymer. The partially epoxidized PS-PI is denoted as PS-PIxn, while *f* and xn (%) represent the mole fraction and degree of epoxidation, respectively.

compositions. A distinctly broader $\mathbf{q}_1$ peak for PS-PI41 indicates a state of disorder. Near extinction of the scattering intensity from PS-PI65 can be attributed to electron density (ρ) matching ($\rho_{PI65} \approx \rho_{PS}$). The effective interaction parameter χ_{eff} between PS and the random copolymer PIxn is estimated from the lamellar periodicity ($d_1 = 2\pi/q_1$) based on self-consistent mean-field field theory (SCFT),[14]

$$d_1 = 1.10aN^{2/3}\chi_{eff}^{1/6} \quad (1)$$

in which the statistical segment length a = 6.53 Å and the degree of polymerization N = 259 are defined based on a common segment volume v = 144 Å^3.[15] Values of χ_{eff} for xn = 0%, 14%, 65%, 75%, and 99% calculated using eq 1 are plotted in Figure 3 (solid symbols); we associate these values with T = 100 °C, approximately the temperature at which the structure is arrested during cooling to room temperature. Although eq 1 is rigorously valid only in the strong segregation limit, prior

Received: August 12, 2011
Accepted: October 19, 2011
Published: November 9, 2011

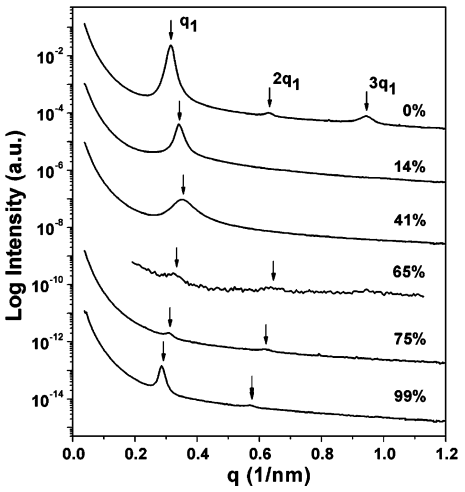

Figure 2. Small angle X-ray scattering (SAXS) obtained from PS-PIxn (with the indicated percentages) at room temperature. Arrows identify discernible Bragg reflections, which are consistent with a lamellar morphology. Data have been shifted vertically for clarity.

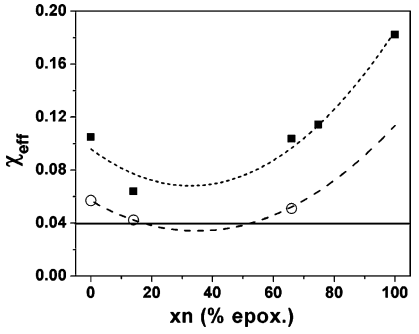

Figure 3. Effective interaction parameter (χ_{eff}) between poly(styrene) and partially epoxidized poly(isoprene) blocks in PS-PIxn diblock copolymers, determined at 100 °C based on d_1 (SAXS data, filled symbols) and T_{ODT} (DMS data, empty symbols). The curves were fit to these points using the binary interaction parameter model (eqs 2 and 3). The solid line identifies the mean-field ODT conditions for N = 259, above and below which the system is ordered and disordered, respectively.

studies[4,16] have shown that this approach yields plausible estimates even close to the order-to-disorder transition (ODT), presumably due to the fluctuation-induced first-order character of the phase transition.[17]

The effective segment−segment interaction parameter for binary blends and block copolymers that contain uniform and random copolymer components can be described by the binary interaction model.[4,18−20] For PS-PIxn,

$$\chi_{eff} = \frac{xn}{100}\chi_{SEI} + \left(1 - \frac{xn}{100}\right)\chi_{SI} - \frac{xn}{100}\left(1 - \frac{xn}{100}\right)\chi_{IEI} \quad (2)$$

where S, I, and EI refer to poly(styrene), poly(isoprene), and epoxidized poly(isoprene) repeat units, respectively. The best fit to eq 2 with the SAXS-based χ_{eff} values (upper curve in Figure 3, where the minimal residual sum of squares = 3.1 × 10^{-4}) yields $\chi_{SI} \approx 0.096$, $\chi_{SEI} \approx 0.19$, and $\chi_{IEI} \approx 0.26$, resulting in a minimum χ_{eff} at xn ≈ 33%. This conclusion is consistent with a report of improved miscibility of poly(styrene) and natural rubber following partial epoxidation[21] and closely resembles the composition dependence of χ_{eff} for partially fluorinated PS-PI diblock copolymers also determined using eqs 1 and 2.[4]

Abrupt changes in the dynamic elastic modulus G' with increasing temperature provided clear evidence of order-to-disorder transition temperatures (T_{ODT}'s) for PS-PI, PS-PI14, and PS-PI65 at 182 °C, 112 °C, and 167 °C, respectively (Figure S7 in the Supporting Information); the other samples showed no sign of an ODT over 85 °C < T < 200 °C. According to mean-field theory, symmetric diblock copolymers are governed by,[22]

$$(\chi N)_{ODT} = 10.5 \quad (3)$$

in which χ is given by eq 1. Generally, the interaction parameter can be expressed as a sum of enthalpic and entropic contributions, where $\chi_{SI} = 28.6T^{-1} - 0.0198$ (corrected for v = 144 Å^3).[23] We assume that χ_{SEI} and χ_{IEI} exhibit the same temperature dependence as χ_{SI}, hence $\chi_{SEI} = k_1\chi_{SI}$ and $\chi_{IEI} = k_2\chi_{SI}$, where k_1 and k_2 are simple proportionality constants. The substitution of these relationships into the binary interaction model yields,

$$\chi_{eff}(xn, T) = \chi_{SI}(T)\left[\frac{xn}{100}k_1 + \left(1 - \frac{xn}{100}\right) - \frac{xn}{100}\left(1 - \frac{xn}{100}\right)k_2\right] \quad (4)$$

Solving eqs 3 and 4 with χ_{eff} (14%, 112 °C) and χ_{eff} (65%, 167 °C) leads to k_1 = 1.99 and k_2 = 3.30. χ_{eff} (xn, 100 °C) is plotted in Figure 3 (lower curve) using these constants. Considering the assumptions and experimental uncertainties associated with these treatments, the SAXS and T_{ODT} derived results are in good agreement. Also shown in Figure 3 is the ODT criterion $\chi_{eff,ODT} = 10.5/N$ (solid line); when $\chi_{eff} > \chi_{eff,ODT}$, the system is predicted to be ordered. Solving eqs 3 and 4 with xn = 41% leads to T_{ODT} = 59 °C, consistent with the SAXS and G' data (i.e., T_{ODT} < 85 °C).

To estimate the changes in surface and interfacial properties of the PIxn domains in the block copolymer as a function of xn, we first investigated the wetting properties of homopolymer films. The dependences of the static contact angle of water (θ_{water}) above cast films of hPIxn (xn = 0%, 15%, 27%, 33%, 79%, 99%) are shown in Figure 4. Measurements of θ_{water} for

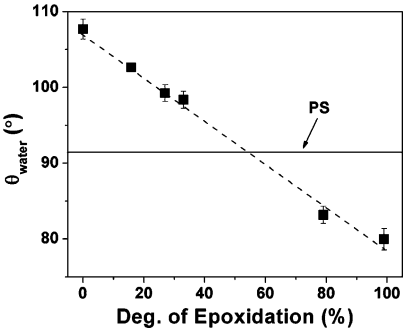

Figure 4. Static contact angle (θ) of water droplets (1 μL) on thin films of hPIxn (filled symbols) and poly(styrene) (hPS) (solid line). Error bars identify standard deviations, and the dashed line illustrates a linear fit to the data.

dx.doi.org/10.1021/mz2000169|ACS Macro Lett. 2012, 1, 11−14

hPI (108°) and hPS (92°) agree with previous reports.[24,25] Increasing the extent of epoxidation reduces θ_{water} for the hPIxn thin films, a trend generally associated with increasing surface energies.[26] Figure 4 suggests that the surface energy of hPIxn is lower than hPS at low degrees of epoxidation, higher than hPS at high degrees of epoxidation, and equals the surface energy of hPS at an intermediate degree of epoxidation. As with many simple liquid mixtures,[27] the surface energy of most copolymers is proportional to the bulk composition (minor deviations from linearity may be explained in terms of sequence distribution and block sizes)[26,28] consistent with the θ_{water} data for hPIxn.

The presentation of PS and PIxn domains in a "fingerprint" pattern at the free surface of a PS-PIxn film (see Figure 5e)

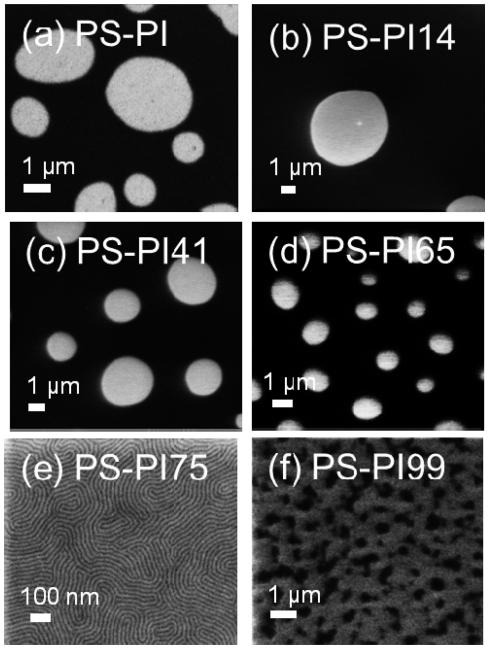

Figure 5. (a–f) Top-down SEM images of PS-PIxn thin films above a cross-linked SMG brush. With one exception, these images contain island and hole textures indicative of a parallel lamellar morphology. A perpendicular lamellar orientation characterizes the film shown in panel e.

confirmed that, at an intermediate degree of epoxidation (xn = 75%), the surface energies of the PS and PI75 blocks are nearly equal at the temperature of annealing. The increase in the surface energy with epoxidation of the random copolymer from γ_{PI} (32.0 mJ/m^2)[29] to the condition that both blocks have nearly equal surface energies, $\gamma_{PI75} \approx \gamma_{PS}$ (40.7 mJ/m^2),[29] agrees with the contact angle measurement. Notably, the fundamental domain period of the perpendicular lamellae, d_1 = 20.3 nm, which is comparable to the smallest dimension feasible with poly(styrene-*b*-methyl methacrylate) diblock copolymer,[30,31] can be reduced roughly 30% for PS-PI75 without inducing disorder based on strong segregation scaling ($d_1 \sim N^{2/3}$) and the results shown in Figure 3.

The results of Figure 5 demonstrate that the interfacial wetting properties of PS-PIxn are also a function of xn. To realize perpendicularly oriented lamellar domains in the PS-PI75 film of thickness 36 nm in Figure 5e, nearly nonpreferential wetting of the blocks of the copolymer at the substrate is required in addition to the condition of nearly equal surface energies. Previously the wetting behavior of substrates toward overlying block copolymer films has been controlled using random copolymer brushes or cross-linked mats of the same[32,33] or different[31,34] combinations of monomers as the block copolymer. Here we find empirically that substrates treated with cross-linked poly(styrene-*ran*-methyl methacrylate) (57 mol % styrene, 37 mol % methyl methacrylate, and 6 mol % glycidyl methacrylate (cross-linker)) mats[33] satisfy the nonpreferential wetting condition at the substrate interface for PS-PI75. Representative SEM images taken from thin films of PS-PIxn (xn = 0, 14, 41, 65, 99) supported on the same composition mats are shown in Figure 5a–d,f. These films contain an "island and hole" texture, indicative of preferred wetting conditions for one of the blocks of the copolymer either at the underlying substrate or at the free surface of the films that orient lamellae parallel to the plane of the film. Preferential block wetting can induce lamellar order in diblock copolymer films that are disordered in the bulk state,[35,36] which may explain the result for sample PS-PI41.

Apparently, the incorporation of a random copolymer molecular architecture in one block of a diblock copolymer (A-*b*-(B-*ran*-C)) decouples the mechanisms that govern bulk phase behavior and surface and interfacial phenomena, a strategy not available to simple (A-*b*-B) diblock copolymers. The parameter χ_{eff}, which governs the bulk (three-dimensional) interactions, depends on χ_{AB}, χ_{AC}, and χ_{BC} interactions and may exhibit a minimum value at intermediate levels of compositions of the random copolymer block. The surface energy of random copolymer block, in contrast, varies approximately linearly with composition between values for pure B and pure C. These different functional forms decouple the bulk and surface thermodynamics allowing neutralization of differences in surface energies of the blocks of the copolymer without disordering the material. For the system studied here, χ_{eff} (xn = 75%) $\approx$ 0.063 while $\gamma_{PI75} \approx \gamma_{PS}$. We believe this decoupling mechanism is a direct consequence of the different roles that a random copolymer molecular architecture plays in the thermodynamics of three-dimensional mixing and demixing versus two-dimensional surface and interfacial phenomena.

Our results show that PS-PIxn phase behavior is quantitatively accounted for by the binary interaction model (eq 2), and the miscibility between PIxn and PS at intermediate compositions is driven by the minimization of strongly unfavorable intramolecular interactions within the statistical copolymer relative to intermolecular interactions, that is, $\chi_{IEI} > \chi_{SI}, \chi_{SEI}$. This model assumes that the probability of segment–segment contact in a completely disordered state is directly proportional to the segment volume fractions. However, "diluting" unfavorable interactions at the two-dimensional surface of a microphase separated block copolymer film may be more restricted than in the three-dimensional bulk state due to the combined effects of polymer chain connectivity and conformational constraints imposed by the microstructure. We believe the concept of controlling the phase-separating and surface properties of block copolymers using random copolymer blocks should be applicable to other monomer combinations, notably those that permit the formation of microphase separated and perpendicularly oriented lamellae (or cylinders) characterized by even smaller domain periods.

■ EXPERIMENTAL SECTION

Size exclusion chromatography (SEC) (Waters 717 Autosampler and Waters 2410 refractive index detector) with tetrahydrofuran (THF) as

the mobile phase was used to determine the number average molecular weight (M_n) and polydispersity index (PDI) of the synthesized polymers; PDI < 1.1 for all PS-PIxn specimens. Proton nuclear magnetic resonance (^{1}H NMR) (VAC-300 Autosampler, IBM Instruments) was utilized to establish the composition of the polymers and to estimate the degree of epoxidation in hPIxn and PS-PIxn.

Random copolymers ($M_n \approx 28.5$ kg/mol, PDI ≈ 1.5) containing styrene (57 mol %), methyl methacrylate (37 mol %), and cross-linkable functional units (6 mol % glycidyl methacrylate), denoted as SMG, were synthesized using nitroxide-mediated living free radical polymerization (NMP).[33] Spin-coating a solution (0.2 wt % in toluene) at 4000 rpm resulted in the formation of a mat, which was cross-linked during 24 h of annealing under vacuum at 190 °C.

Isochronal (ω = 1 rad/s) linear dynamic mechanical spectroscopy (DMS) was conducted on pressed PS-PIxn samples with an ARES rheometer (Rheometric Scientific). SAXS experiments were conducted at room temperature on PS-PIxn specimens at the Argonne National Laboratory and on a laboratory source (Materials Science Center (MSC) at the Univ. of Wisconsin at Madison) after annealing in vacuum at 105 °C for 6 h. Data collected on an area detector were reduced to the one-dimensional form of intensity versus scattering wavevector magnitude $q = 4\pi\lambda^{-1}\sin(\theta/2)$.

Solutions of PS-PIxn (1.0 wt %, in toluene) were spin-coated on the cross-linked brushes with average film thicknesses ranging from $1.7d_1$ to $1.9d_1$ ($d_1 = 2\pi/q_1$ where q_1 is the principle Bragg reflection measured by SAXS; AutoEL-II, Rudolph Research). The thin films were annealed at 107 °C for 6 h in vacuum and characterized by scanning electron microscopy (SEM) (LEO 1550-VP FESEM). Twenty-two 30 nm thick films of hPS and hPIxn, 22 to 30 nm thick, were produced by spin coating above bare Si wafers. Static contact angles formed by a drop of water (1 μL) at the thin film surface (averaged over 5−10 measurements) were established using a goniometer (Data Physics OCA15).

■ ASSOCIATED CONTENT

Supporting Information

(1) Sample preparation method, (2) table of molecular characterization of hPS, hPI, and PS-PIxn, (3) table of lamellar periodicities and T_{ODT}'s of PS-PIxn, (4) SEC and DSC traces of hPIxn and PS-PIxn, and (5) ^{1}H NMR and isochronal and isothermal rheology data of PS-PIxn. This material is available free of charge via the Internet at http://pubs.acs.org.

■ AUTHOR INFORMATION

Corresponding Author

*E-mail: bates001@umn.edu.

Notes

The authors declare no competing financial interest.

■ ACKNOWLEDGMENTS

Financial support for this work was provided by the Nanoscale Science and Engineering Center (NSEC). The authors thank Chris Thode for providing the cross-linkable brush material and Christopher M. Bates for helpful comments on the manuscript.

■ REFERENCES

(1) Bates, F. S.; Fredrickson, G. H.; Hucul, D.; Hahn, S. F. *AIChE J.* **2001**, *47* (4), 762−765.
(2) Odian, G. *Principles of Polymerization*, 4th ed.; Wiley Interscience: Hoboken, NJ, 2004.
(3) Bates, F. S.; Fredrickson, G. H. *Phys. Today* **1999**, *52* (2), 32−38.
(4) Ren, Y.; Lodge, T. P.; Hillmyer, M. A. *Macromolecules* **2000**, *33* (3), 866−876.
(5) Davidock, D. A.; Hillmyer, M. A.; Lodge, T. P. *Macromolecules* **2004**, *37* (2), 397−407.
(6) Kimishima, I.; Jinnai, H.; Hashimoto, T. *Macromolecules* **1999**, *32* (8), 2585−2596.
(7) Grubbs, R. B.; Dean, J. M.; Broz, M. E.; Bates, F. S. *Macromolecules* **2000**, *33* (26), 9522−9534.
(8) Verploegen, E.; Zhang, T.; Murlo, N.; Hammond, P. T. *Soft Matter* **2008**, *4* (6), 1279−1287.
(9) Tanrattanakul, V.; Wattanathai, B.; Tiangjunya, A.; Muhamud, P. *J. Appl. Polym. Sci.* **2003**, *90* (1), 261−269.
(10) Brosse, J. C.; Campistron, I.; Derouet, D.; El Hamdaoui, A.; Houdayer, S.; Reyx, D.; Ritoit-Gillier, S. *J. Appl. Polym. Sci.* **2000**, *78* (8), 1461−1477.
(11) Nikje, M. M. A.; Rafiee, A.; Haghshenas, A. *Des. Monomers Polym.* **2006**, *9* (3), 293−303.
(12) Hayashi, O.; Takahashi, T.; Kurihara, H.; Ueno, H. *Polym. J.* **1981**, *13* (3), 215−223.
(13) Bradbury, J. H.; Perera, M. C. S. *J. Appl. Polym. Sci.* **1985**, *30* (8), 3347−3364.
(14) Semenov, A. N. *Sov. Phys. JETP* **1985**, *61*, 733.
(15) Fetters, L. J.; Lohse, D. J.; Richter, D.; Witten, T. A.; Zirkel, A. *Macromolecules* **1994**, *27* (17), 4639−4647.
(16) Almdal, K.; Rosedale, J. H.; Bates, F. S.; Wignall, G. D.; Fredrickson, G. H. *Phys. Rev. Lett.* **1990**, *65* (9), 1112−1115.
(17) Bates, F. S.; Rosedale, J. H.; Fredrickson, G. H.; Glinka, C. J. *Phys. Rev. Lett.* **1988**, *61* (19), 2229−2232.
(18) Roe, R. J.; Zin, W. C. *Macromolecules* **1980**, *13* (5), 1221−1228.
(19) ten Brinke, G.; Karasz, F. E.; Macknight, W. J. *Macromolecules* **1983**, *16* (12), 1827−1832.
(20) Kambour, R. P.; Bendler, J. T.; Bopp, R. C. *Macromolecules* **1983**, *16* (5), 753−757.
(21) Chuayjujit, S.; Sakulkijpiboon, S.; Potiyaraj, P. *Polym. Polym. Comp.* **2010**, *18* (3), 139−144.
(22) Fredrickson, G. H.; Helfand, E. *J. Chem. Phys.* **1987**, *87* (1), 697−705.
(23) Lodge, T. P.; Pan, C.; Jin, X.; Liu, Z.; Zhao, J.; Maurer, W. W.; Bates, F. S. *J. Polym. Sci., Part B: Polym. Phys.* **1995**, *33* (16), 2289−2293.
(24) Lee, L. H. *J. Polym. Sci., Part B: Polym. Phys.* **1967**, *5*, 1103−1118.
(25) Wu, S. *J. Polym. Sci., Part C: Polym. Symp.* **1971**, *34*, 19−30.
(26) Adao, M. H. V. C.; Saramago, B. J. V.; Fernandes, A. C. *J. Colloid Interface Sci.* **1999**, *217* (1), 94−106.
(27) Morgan, J. L. R.; Neidle, M. *J. Am. Chem. Soc.* **1913**, *35* (12), 1856−1865.
(28) Donley, J. P.; Fredrickson, G. H. *Macromolecules* **1994**, *27* (2), 458−467.
(29) Brandrup, J.; Immergut, E. H. *Polymer Handbook*; John Wiley & Sons: New York, 1999.
(30) Hinsberg, W.; Cheng, J.; Kim, H.; Sanders, D. P. *Proc. SPIE* **2010**, *7637*, 76370G.
(31) Cheng, J. Y.; Rettner, C. T.; Sanders, D. P.; Kim, H. C.; Hinsberg, W. D. *Adv. Mater.* **2008**, *20* (16), 3155−3158.
(32) Mansky, P.; Liu, Y.; Huang, E.; Russell, T. P.; Hawker, C. J. *Science* **1997**, *275* (5305), 1458−1460.
(33) Han, E.; Stuen, K. O.; La, Y. H.; Nealey, P. F.; Gopalan, P. *Macromolecules* **2008**, *41* (23), 9090−9097.
(34) Bates, C. M.; Strahan, J. R.; Santos, L. J.; Mueller, B. K.; Bamgbade, B. O.; Lee, J. A.; Katzenstein, J. M.; Ellison, C. J.; Willson, C. G. *Langmuir* **2011**, *27* (5), 2000−2006.
(35) Mansky, P.; Tsui, O. K. C.; Russell, T. P.; Gallot, Y. *Macromolecules* **1999**, *32* (15), 4832−4837.
(36) Foster, M. D.; Sikka, M.; Singh, N.; Bates, F. S.; Satija, S. K.; Majkrzak, C. F. *J. Chem. Phys.* **1992**, *96* (11), 8605−8615.